Spin Solar Cell Phenomenon on Single Molecule Magnet(SMM) Impacted CoFeB based Magnetic Tunnel Junctions

Marzieh Savadkoohi [1,2], Daniel Gopman[2], Pius Suh, Carlos Rojas-Dotti,[3] José Martínez-Lillo,*[3] Pawan Tyagi*[1]
Mechanical Engineering, University of the District of Columbia [1],
Materials Science and Engineering Division, National Institute of Standards and Technology, Gaithersburg [2]
Departament de Química Inorgànica / Instituto de Ciencia Molecular (ICMol), University of Valencia, Spain [3]

ABSTRACT: The single-molecule magnet (SMM) transformed conventional magnetic tunnel junction(MTJ), a memory device used in present-day computers, into solar cells. For the first time, we demonstrated the electronic spin-dependent solar cell effect on an SMM-transformed MTJ under unpolarized white light. In our MTJ, CoFeB was present on both sides of the MgO tunnel barrier. We produced cross-junction-shaped MTJ with the two exposed junction edges where the physical gap between two electrodes was less than the length of to-be-bridged SMM spin channels. Along the exposed edges we bridged SMM between the two CoFeB electrodes across the insulating barrier and observed that SMM channels yielded a region of long-range magnetic ordering around molecular junctions. Our SMM possessed a hexanuclear $[Mn_6(\mu_3\text{-}O)_2(H_2N\text{-}sao)_6(6\text{-}atha)_2(EtOH)_6]$ [H_2N-saoH = salicylamidoxime, 6-atha = 6-acetylthiohexanoate] complex and thiols end groups to form bonds with metal films. SMM impacted MTJ started exhibiting the solar cell effect and yielded ≈80 mV open circuit voltage and ≈10mA/Sq.cm saturation current under one sun radiation. Kelvin Probe AFM(KPAFM) study provided direct evidence that SMM has transformed the electronic properties of the MTJ's electrodes over several thousand times more areas as compared to molecular junctions area at room temperature.

Keywords: Spin; SMM; MTJ; Solar Cell; PV

INTRODUCTION:

Spintronics is the utilization of spins degree of freedom to produce novel functionalities such as quantum computing, neuromorphic computing, high storage density, non-volatile Random-Access Memories (MRAMs), etc [1]. The field of solar cells has found a connection with spintronics[2]. The solar cell field has been conventionally focused on electron charge property, and electron spin has no role in solar electricity generation. In the last two decades, a number of intriguing electrons spin-dependent solar cell observations have been reported [2]. Electron spin has been demonstrated to play a direct role in the light absorption mechanism and in the establishment of an analog of built-in potential to drive change through the desired load. Researchers have used different approaches to study spin photovoltaic effects to improve solar cells' yield and efficiency. Conventional charge-based p-n junctions [3], quantum wires and nanoscale channels, and metal/nonmagnetic semiconductor systems [4] are a variety of platforms used for observing spin photovoltaic or spin solar cell effect [2a, 5]. These

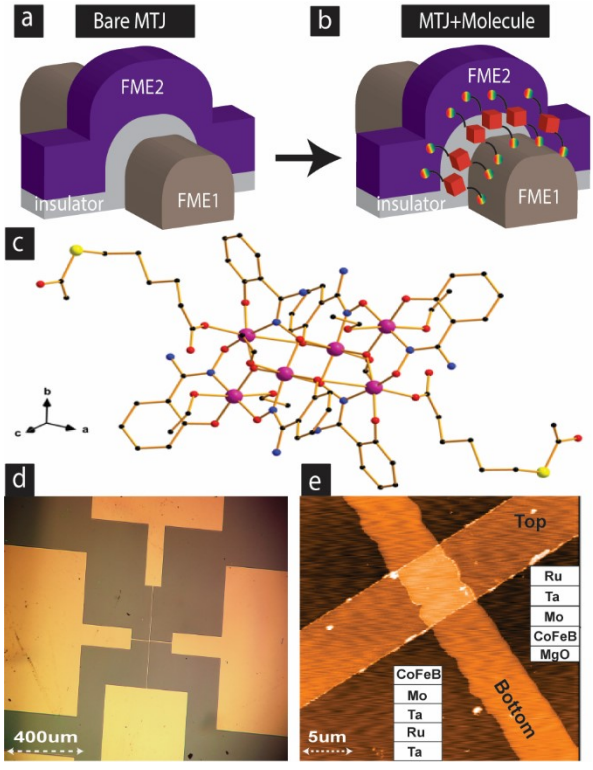

Figure 1: MTJMSD configuration (a) Bare and, (b) After molecular treatment. (c) Single-Molecule Magnet (SMM) structure (d) Optical microscope image of MTJMSC's cross junction (e) AFM scan of MTJMSD's cross junction

different approaches bring a variety of mechanisms to engage electron spin in light absorption and photovoltaic effect. However, none of the experimental studies have progressed from the initial observations state and suffer from several limitations.

Recently, molecular spintronics devices have been reported to show the solar cell phenomenon under regular unpolarized light radiation, and the mechanism was focused on C_{60} molecule and ferromagnetic interfaces [6]. In our prior work, we demonstrated the spin-dependent solar cell effect on magnetic tunnel junction (MTJ) based molecular spintronics device (MTJMSD) architecture [7]. For the first time, we observed that paramagnetic molecules transformed ferromagnetic NiFe electrodes into semiconducting material that responded to light. Prior MTJMSD utilized NiFe/AlOx/NiFe/Co MTJ structure[8] and S=6 cyanide-bridged octanuclear (Fe4Ni4II)-Ni-III complex paramagnetic molecules[9]. In this case, paramagnetic molecular channels themselves did not absorb light. However, they transformed the ferromagnetic electrodes (FME) in such a way the MTJ started showing p-n junction diode-like transport characteristics [7]. However, this study created critical questions, If the MTJMSD-based solar cell phenomenon, is limited to the reported combination of MTJ and (Fe4Ni4II)-Ni-III complex molecules [9]. Another critical question was about the effect of MTJ thin film configurations. It is noteworthy that we did not see the spin photovoltaic effect on MTJ with identical ferromagnetic electrodes [10]. We hypothesized that significant dissimilar ferromagnetic electrodes are necessary to see molecule-based spin photovoltaic effect. In this paper, we investigate CoFeB and MgO-based MTJ. Here, we report the observation of the solar cell effect on the MTJMSD involving MTJ with regularly utilized thin film stack configuration in MTJ based memory devices. This paper also reports intriguing observation of large-scale ordering produced by the SMM molecular channels on MTJ ferromagnetic electrodes.

EXPERIMENTAL DETAILS: We explored SMM as another category of molecular channel [10](Fig.1c). This molecule was successfully utilized in forming MTJMSD. We have used cross-junction-shaped isolated MTJs to minimize interference from neighboring devices (Fig. 1d). To observe the photovoltaic effect, MTJ was deposited with the following thin film configuration: Ta(5nm)/Ru(8nm)/Ta(5nm)/Mo(1nm)/CoFeB(6nm)/MgO(2nm)/CoFeB(4nm)/Mo(1nm)/Ta(5nm)/Ru(8nm on a silicon wafer with 300 nm silicon dioxide layer (Fig.1e). MTJMSD fabrication consisted of i) photolithography on the substrate to define the bottom electrode dimensions ii) deposition of the Ta(5nm)/Ru(8nm)/Ta(5nm)/Mo(1nm)/CoFeB(6nm) bottom electrode, iii) lift-off, iv) photolithography for the insulator and thin top electrode cavity perpendicular to the bottom electrode, v) deposition of MgO, top CoFeB ferromagnet and capping layers and iii) magnetic molecules' attachment to the top and bottom electrode through a self-assembly electrochemical process (fig 1(a,b)). The optical and atomic force microscopy (AFM) images in figure 1(c-d) represent one MTJMSD cross junction of about ≈20 μm^2 area fabricated with the explained strategy. Detailed experimental fabrication details are described elsewhere [8, 10]

RESULTS AND DISCUSSION:

Figure.2a shows an IV measurement of an MTJ before and after hosting SMM (Fig. 1c) molecular channels along the exposed sides to become MTJMSD (Fig. 1b). This transport study was performed under the room light. We did not see any effect of light on the bare tunnel junction in multiple studies (Fig. 2a), as indicated by the symmetric I-V that intersects zero voltage at zero current. However, within a few hours after establishing the SMM channel, two phenomena happened. MTJMSD settled in the suppressed current state, not observable in Fig. 2a due to ≈the 1000-fold difference in current magnitude, and also started showing solar cell effect (Fig. 2b). In the dark, MTJMSD current-voltage resembles diode characteristics (Fig. 2b). Under room light MTJMSD showed ≈3 nA saturation current and ≈80 mV open circuit voltage (Inset, Fig. 2b). Our results show that the photovoltaic effect in MTJMSD's initial state under 100 ≈ (Fig. 2b) was comparable to the PV effect in two weeks aged MTJMSD

under 700 W/m^2 (Fig. 2c). It is noteworthy that the 100 W/m^2 measurement was performed right after molecular treatment when MTJMSD had not reached to its equilibrium state yet. Two weeks gap between SMM treatment and solar cell characterization (Fig. 2c) was believed to produce more ordered ferromagnetic electrodes under strong antiferromagnetic coupling between FMEs. Temporal stabilization has been observed to produce different magnetic phases leading to various forms of photovoltaic effect in the previous study by our group [7].

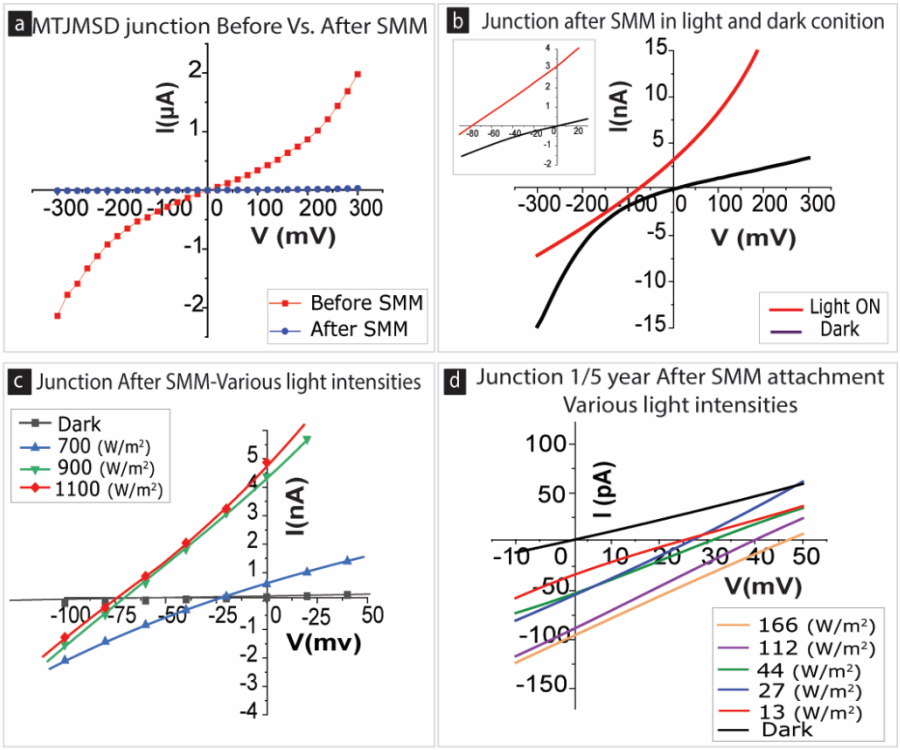

Figure 2: MTJMSD's cross junction IV measurement (a) before vs. after molecular treatment (b) in dark and light condition (c) under different light intensities after two weeks (d) observing PV effect under various light intensities after 1/5 year.

However, the solar effect varied with time. We observe that as MTJMSD stabilized, further solar cell effect varied with respect to observation in the initial stage (Fig. 2c). MTJMSD solar electricity generation was tested under a solar simulator ≈two weeks after fabrication. Saturation current and open circuit voltage differed significantly when light intensity increased up to 900 W/m^2 (Fig. 2c). However, no further enhancement occurred when light intensity increased from 900 to 1100 W/m^2. We also investigated the effect of aging on photovoltaic effect by studying the transport study in dark and light after 1.5 year. We observed that MTJ transport settled into more suppressed current state in pA range and junction responded to light exposure (Fig. 2d). In general, increasing white light intensity increased the photocurrent and open circuit voltage (Fig. 2d).

We also considered the possibility of the MTJMSD bottom electrode getting oxidized even during the fabrication state and then started showing unstable behavior with time. According to the literature, oxidized metals such as Cu_2O, WO_x, and FeO can produce the photovoltaic effect and were used in forming complete solar cells [4d, 11]. Oxidized metals' optical properties, such as light reflection scattering and absorption, can be different than bare metals [12]. Our second photolithography step consists of coating the bottom electrode with photoresist and baking that at 90 °C. Baking of a photoresist-covered bottom electrode with a CoFeB layer on top could undergo oxidation and change the bottom electrode's electric and magnetic properties. To make sure that the observed P.V. effect is not due to oxidation at the baking step, we did a controlled study with a reflectometer (Supplementary material Figure S1). To do so, MTJ was deposited up to the CoFeB layer on the bottom electrode, exposed to various temperatures for 30 minutes, and cooled down to room temperature for optical measurement. The goal was to track CoFeB's reflectance spectra evolving with increasing temperature. If oxidation happens, we could have witnessed a significant change in reflectance signal intensity after a

certain annealing temperature. However, our results showed that CoFeB optical characteristics remain intact between room temperature (R.T.) and 100 $°C$, and major changes started to occur at higher temperature values.

We hypothesized that strong molecule-induced exchange coupling has to create the necessary properties in the ferromagnetic electrodes to absorb sufficient solar radiation. Molecules in the MTJMSD itself are in the 0.001 µm x 4 µm =0.004 µm2 area. The molecule channel area around the two edges is ≈10,000 smaller than the ≈20 μm^2 junction area. An estimate of power generation/unit area with molecular channel area leads to an unrealistic situation. If molecular junctions' local area is included in the calculation, then power production turns out to be ≈100 times more than what was inputted on the junction, and that is not possible. Hence, we believe that the photovoltaic effect is arising from the areas in and around the tunnel junction.

We postulated that if SMM produced a room temperature stable photovoltaic effect, then it must have created room temperature stable long-range impact that can be observed in microscopy. To gain an in-depth understanding, we conducted Kelvin Probe Force Microscopy (KPFM) on MTJMSD's junction before and after molecules treatment. On the bare MTJ before SMM treatment, KPAFM exhibited similar results for the top and bottom electrodes (Fig. 3a). Interestingly, we observed a stark change in ferromagnetic electrodes' surface potential after SMM attachment at room temperature. We observed the appearance of multiple phases in the top electrode (Fig. 3b) that were absent in the bare state of MTJ (Fig. 3a). The appearance of multiple phases is expected to be a built-in potential presence around the junction area. In our recent research on the anisotropy effect, we have discussed the role of voltage-induced anisotropy producing multiple phases on MTJMSD's magnetic electrode [13]. Interestingly, unlike the top electrode, the bottom electrode exhibited a very stable surface potential over a long range (Fig. 3b). Bottom electrode stack Ta/Ru/Ta/Mo/CoFeB

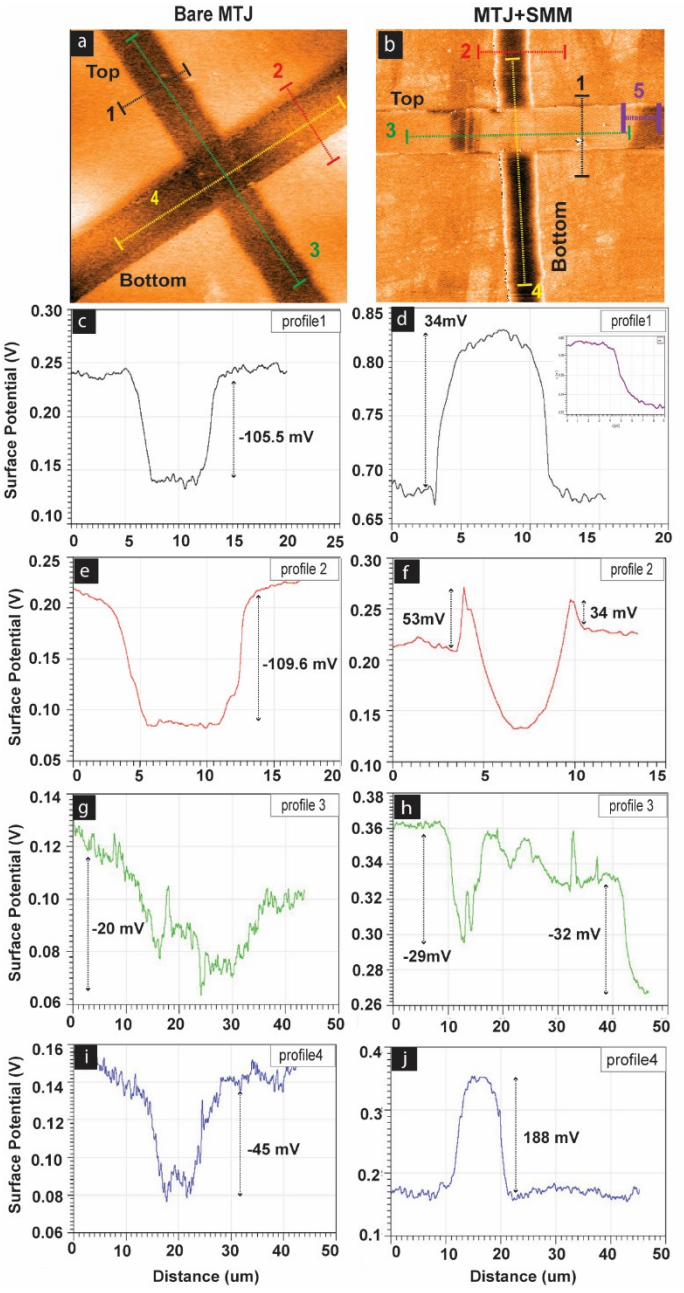

Figure 3: KPFM scan of MTJMSD's cross junction (a) before attaching molecules (b) after attaching molecule; (c-d) Surface potential of top electrode before Vs. after SMMs (e-f) Surface potential of bottom electrode before Vs. after SMMs; (g-h) difference between top and bottom electrode surface potential before and after SMM treatment along the length of electrodes; (i-j) difference between the top and bottom electrode before and after transforming bare MTJ into MTJMSD via molecule treatment

was impacted in the whole area of observation that was at least ≈10 times more than cross junction area (Fig. 3b). Based on the experimentally observed long-range impact, especially on the bottom electrode, we concluded that molecules impacted beyond the junction area where molecules bonded with the two electrodes (Fig. 1b and e). Hence, it is highly likely that the light active region is associated with the impacted ferromagnetic electrodes, not the local region where molecules are chemically bonded to the two electrodes along the two sides of the MTJ. Our current conclusion from this KPAFM is consistent with MFM and KPAFM study performed on MTJMSD involving MTJ with Co/NiFe/AlOx/NiFe configuration and OMC molecules [7]. It is noteworthy that OMC paramagnetic molecule [7] differs from the SMM used in this study (Fig.1c).

We further investigated the SMM impact by focusing on different parts of the MTJ and MTJMSD along the line profiles indicated in Figures 3a and b. Line profile 1 on bare MTJ shows that the top electrode surface potential is 105±9 mV lower than that of the substrate (Fig. 3c). Interestingly, the line profile-1 on MTJMSD (Fig. 3d) shows that the top electrode surface potential was 130±17 mV higher than that of the substrate (Fig. 3d). The top electrode surface potential after the molecule treatment changed from -105 mV to +130 mV with respect to the substrate after molecule bridging. The molecule has produced ≈235 mV difference on top electrode. Interestingly, line profile 5 on MTJMSD's top electrode exhibited different surface potential in the two phases (Inset Fig. 3d), and this difference was 32±1 mV. We were also curious about the surface potential of the different phases on the bottom electrode of MTJMSD.

We further investigated the surface potential of the bottom electrode of MTJ (Line profile 2-Fig. 3a) and MTJMSD (Line profile 2 -Fig.3b). Surface potential along the line profile 2 on the bottom electrode was 110±15 mV lower than the substrate (Fig. 3e). The potential surface profile on the bottom electrode before SMM treatment (Fig.3e) was similar to the analogous profile on top electrode before SMM treatment (Fig. 3c). The difference between top and bottom electrode difference was ≈5 mV. However, the potential profile on the bottom electrode of MTJMSD (Fig. 3f) was starkly different as compared to the potential surface profile of the bottom electrode before the SMM treatment (Fig. 3e). Along the line profile2 (Fig.3b), the bottom surface potential profile was different around the electrode edge as compared the center (Fig. 3f). Interestingly, bottom electrode surface potential near the edges was more than that of substrate's surface potential (Fig. 3f). Bottom electrode edge surface potential was 34±2 mV more than the substrate potential (Fig. 3f). However, the surface potential in the middle of the electrode was 29±1 mV lower with respect to the substrate potential.

We also compared the difference between top and bottom electrode surface potential before and after SMM treatment along the length of electrodes to observe the variations. The line profile 3 on bare MTJ before the molecule is shown (Fig. 3g). There is an average change of ≈20 mV along the length (Fig.3 g), and ≈5 mV perturbation around the junction area was observed (Fig. 3g). However, line profile 3 along the MTJMSD top electrode showed major perturbations at the sites of phase changes (Fig. 3h). The local perturbation at the site of left phase change was ≈29 mV, and right side of the phase change was ≈32 mV (Fig. 3h). To estimate the difference between the top and bottom electrode before and after transforming bare MTJ into MTJMSD via molecule treatment we studied on line profile 4 (Fig. i-j). The difference between the top and bottom electrodes before SMM treatment along the line4 profile was 45±4 mV; the top electrode potential was lower than the bottom electrode (Fig. 3i). However, the difference between top and bottom electrodes after SMM treatment along the line4 profile was 188±10 mV. It is remarkable the molecule bridging along the edges has resulted in an increase in potential difference from -45 mV to ≈188 mV, that amount to ≈230 mV. Based on our prior knowledge of the related device, the long-range impact on electrode potential is associated with the molecule-induced strong antiferromagnetic coupling leading to the dramatic change in the spin density of states. Unfortunately, the current device structure with a nonmagnetic layer and very thin magnetic layers was difficult to study by other spectroscopies like MFM.

It is noteworthy that built-in potential generation in conventional p-n junction solar cells is directly associated with the difference in contact potential of the p and n regions [14]. We hypothesized that SMM's ability to produce a room-temperature stable large difference in contact potential between the top and the bottom electrode is producing an analogous built-in potential. However, unlike p-n junction solar cells where doping concentration yields the built-in potential, MTJMSD's built-in potential is solely due to the interaction of molecule spin with the two ferromagnetic electrodes. We also demonstrated previously that molecule-affected ferromagnetic electrodes in the MTJMSD junction area were able to absorb the light radiation [7]. We surmise that SMM-produced room temperature stable phases are light sensitive and similar to semiconductors, have an energy gap. However, we are unable to provide an exact estimation of the energy gap between spin-related conduction and spin-related valance bands due to limited resources and complexity in MTJMSD geometry. Since light absorption and built-in potential in an MTJMSD is due to the spin interactions of SMM molecules and magnetic electrode, we termed MTJMSD's photovoltaic effect as the spin photovoltaic effect.

CONCLUSION: Magnetic tunnel junction-based molecular spintronics devices (MTJMSD) can be used as a testbed for spin-current generation. We observed that a CoFeB/MgO/CoFeB based-MTJMSD shows a photovoltaic effect after single-molecule magnets (SMM) attachment along the exposed side edges. About 50% of our device junctions showed a photovoltaic effect under regular white light. However, open circuit voltage and saturation current changed over a period of one and a half years. According to our theoretical simulation, MTJMSD keeps stabilizing with time, and freshly made MTJMSD's magnetic properties differ from that after a long time. KPAFM has provided unique insights and suggests the contact potential on MTJMSD is a strong function of magnetic tunnel junction's ferromagnetic electrodes' properties. SMM used in this study did not produce any photovoltaic effect on nickel electrodes. Our KPAFM study also showed that the contact potential on the two electrodes of the MTJMSD was opposite and suggested the presence of a built-in potential causing the separation of photo-generated electrons in molecule impacted electrode. This work is consistent with the spin-photovoltaic effect observed on Co/NiFe/AlOx/NiFe and organometallic molecular cluster (OMC) based MTJMSDs. Future studies will focus on attempting different types of MTJ with a wide range of magnetic electrodes and molecule combinations to understand the exact mechanism and optimize solar cell performance. We were unable to estimate efficiency because of the lack of knowledge about the area involved in solar electricity generation, which will be the focus of future work. The most exciting outcome of this research is that one can use earth-abundant Co, Fe, and Ni-like ferromagnetic materials for electricity generation. This work provides motivation for collaboration between MTJ researchers and chemists to explore the spin-photovoltaic and vast range of novel phenomena that can only be observed via the MTJMSD method.

ACKNOWLEDGMENTS:

We gratefully acknowledge the funding support, which was in part supported by the National Science Foundation-CREST Award (Contract No. HRD-1914751), Department of Energy/National Nuclear Security Agency (DE-FOA-0003945). This research was also funded by the Spanish Ministry of Science and Innovation [Grant numbers PID2019-109735GB-I00 and CEX2019-000919-M (Excellence Unit "María de Maeztu")] and Generalitat Valenciana [Grant number AICO/2021/295]. M.S. conducted experiments under the supervision of P.T. and D.G. P.S. did control experiments. CRD and JML synthesized the molecules. P.T. and M.S. wrote the manuscript that was edited by all the coauthors.

Competing interests

The authors have no relevant financial or non-financial interests to disclose.

Availability of data and material

Data used in this paper is available upon request.

Ethical Compliance: There is no human subject involvement.

REFERENCES:

1. Hirohata, A.; Yamada, K.; Nakatani, Y.; Prejbeanu, I.-L.; Diény, B.; Pirro, P.; Hillebrands, B., Review on spintronics: Principles and device applications. *Journal of Magnetism and Magnetic Materials* **2020,** *509*, 166711.
2. (a) Sun, X.; Vélez, S.; Atxabal, A.; Bedoya-Pinto, A.; Parui, S.; Zhu, X.; Llopis, R.; Casanova, F.; Hueso, L. E., A molecular spin-photovoltaic device. *Science* **2017,** *357* (6352), 677-680; (b) Wang, J.; Lu, H.; Pan, X.; Xu, J.; Liu, H.; Liu, X.; Khanal, D. R.; Toney, M. F.; Beard, M. C.; Vardeny, Z. V., Spin-Dependent Photovoltaic and Photogalvanic Responses of Optoelectronic Devices Based on Chiral Two-Dimensional Hybrid Organic–Inorganic Perovskites. *ACS Nano* **2021,** *15* (1), 588-595; (c) Xu, H.; Wang, H.; Zhou, J.; Li, J., Pure spin photocurrent in non-centrosymmetric crystals: bulk spin photovoltaic effect. *Nature Communications* **2021,** *12* (1), 4330.
3. (a) Fabian, J., Spin-voltaic effect and its implications. *Materials Transactions* **2003,** *44* (10), 2062-2065; (b) Endres, B.; Ciorga, M.; Schmid, M.; Utz, M.; Bougeard, D.; Weiss, D.; Bayreuther, G.; Back, C., Demonstration of the spin solar cell and spin photodiode effect. *Nature communications* **2013,** *4* (1), 2068; (c) Kondo, T.; Hayafuji, J.-j.; Munekata, H., Investigation of spin voltaic effect in ap–n heterojunction. *Japanese journal of applied physics* **2006,** *45* (7L), L663.
4. (a) Hekking, F.; Nazarov, Y. V., Photovoltaic effect in quantum adiabatic transport as a way to pump electrons. *Physical Review B* **1991,** *44* (20), 11506; (b) Pershin, Y. V.; Piermarocchi, C., Photovoltaic effect in bent quantum wires in the ballistic transport regime. *Physical Review B* **2005,** *72* (19), 195340; (c) Fedorov, A.; Pershin, Y. V.; Piermarocchi, C., Spin-photovoltaic effect in quantum wires due to intersubband transitions. *Physical Review B* **2005,** *72* (24), 245327; (d) Fedichkin, L.; Ryzhii, V.; V'yurkov, V., The photovoltaic effect in non-uniform quantum wires. *Journal of Physics: Condensed Matter* **1993,** *5* (33), 6091.
5. Bottegoni, F.; Celebrano, M.; Bollani, M.; Biagioni, P.; Isella, G.; Ciccacci, F.; Finazzi, M., Spin voltage generation through optical excitation of complementary spin populations. *Nature materials* **2014,** *13* (8), 790-795.
6. Sun, X. N.; Velez, S.; Atxabal, A.; Bedoya-Pinto, A.; Parui, S.; Zhu, X. W.; Llopis, R.; Casanova, F.; Hueso, L. E., A molecular spin-photovoltaic device. *Science* **2017,** *357* (6352), 677-+.
7. Tyagi, P.; Riso, C., Molecular spintronics devices exhibiting properties of a solar cell. *Nanotechnology* **2019,** *30* (49), 495401.
8. Tyagi, P.; Riso, C.; Friebe, E., Magnetic Tunnel Junction Based Molecular Spintronics Devices Exhibiting Current Suppression At Room Temperature. *Organic Electronics* **2019,** *64*, 188-194.
9. Li, D. F.; Parkin, S.; Wang, G. B.; Yee, G. T.; Clerac, R.; Wernsdorfer, W.; Holmes, S. M., An S=6 cyanide-bridged octanuclear (Fe4Ni4II)-Ni-III complex that exhibits slow relaxation of the magnetization. *J. Am. Chem. Soc.* **2006,** *128* (13), 4214-4215.
10. Tyagi, P.; Riso, C.; Amir, U.; Rojas-Dotti, C.; Martínez-Lillo, J., Exploring room-temperature transport of single-molecule magnet-based molecular spintronics devices using the magnetic tunnel junction as a device platform. *RSC Advances* **2020,** *10* (22), 13006-13015.
11. (a) O'Dell, J. Cheap solar panels could be made from oxidized metals. https://venturebeat.com/enterprise/cheap-solar-panels-could-be-made-from-oxidized-metals/; (b) Tran, T. A.; Trinh, T. T.; Viet, T. D.; Do, H. B.; Giang, N. T. T.; Kim, S.; Pham, D. P.; Yi, J.; Dao, V.-A., Effects of oxidation state on photovoltaic properties of reactively magnetron sputtered hole-selective WOx contacts in silicon heterojunction solar cells. *Semiconductor Science and Technology* **2020,** *35* (4),

045020; (c) Ameur, A.; Berrada, A.; Loudiyi, K.; Adomatis, R., Performance and energetic modeling of hybrid P.V. systems coupled with battery energy storage. In *Hybrid Energy System Models*, Elsevier: 2021; pp 195-238.
12. (a) Leberknight, C. E.; Lustman, B., An Optical Investigation of Oxide Films on Metals. *J. Opt. Soc. Am.* **1939,** *29* (2), 59-66; (b) Blewett, D. T.; Cahill, J. T.; Lawrence, S. J.; Denevi, B. W.; Nguyen, N. V., Iron metal optical constants: Assessing the effects of metal composition and oxidation on laboratory reflectance spectra of planetary materials. 2012; Vol. 2012, pp P12A-06.
13. Dahal, B. R.; Savadkoohi, M.; Grizzle, A.; D'Angelo, C.; Lamberti, V.; Tyagi, P., Easy axis anisotropy creating high contrast magnetic zones on magnetic tunnel junctions based molecular spintronics devices (MTJMSD). *Scientific reports* **2022,** *12* (1), 1-14.
14. (a) Kittel, C., *Intorduction to Solid State Physics*. 7th ed.; John Wiley & Sons, Inc: New York, 1996; (b) Polak, L.; Wijngaarden, R. J., Two competing interpretations of Kelvin probe force microscopy on semiconductors put to test. *Physical Review B* **2016,** *93* (19), 195320.